# Synergy theory in radiobiology

Dae Woong Ham[3], Binglin Song[1], Jian Gao[3], Julien Yu[3], and Rainer K. Sachs[1,2]

[1] Department of Mathematics, University of California at Berkeley

[2] Corresponding Author, Rainer K. Sachs, sachs@math.berkeley.edu, 510-658-5790

[3] Department of Statistics, University of California at Berkeley

**Abstract**

Customized open-source software is used to characterize, exemplify, compare and critically evaluate mathematical/computational synergy analysis methods currently used in biology and used or potentially applicable in radiobiology. As examples, we reanalyze published results on murine tumors and on *in vitro* chromosome aberrations induced by exposure to single-ion beams that simulate components of the galactic cosmic ray radiation field. Baseline no-synergy/no-antagonism mixture dose-effect relations are calculated for corresponding mixed beams. No new experimental results are presented.

Synergy analysis of effects due to a mixed radiation field whose components' individual dose-effect relations are highly curvilinear should not consist of simply comparing to the sum of the components' effects. Such curvilinearity must often be allowed for in current radiobiology, especially when studying possible non-targeted ('bystander') effects. Analyzing synergy via incremental effect additivity is then preferable to using the simple effect additivity theory.

Systematic synergy analysis methods, including statistical significance estimates, are available even when pronounced individual dose-response relation curvilinearity is a confounding factor, and are useful. However, synergy theory has substantial limitations that have sometimes been glossed over. Each of many specific competing synergy theory approaches has in addition its own limitations that should be taken into account.

## 1. Introduction

Ionizing radiation fields are often mixed rather than involving just one radiation quality. More generally, agent mixtures, e.g. mixtures of therapeutic drugs or of toxins, are important in biology. Typically the main information on the mixture components is their individual dose-effect relations (IDERs) and one wants to know when mixture data indicate synergy, antagonism, or neither. This is often done by comparing an observed mixture dose effect relation (MIXDER) with a baseline MIXDER defining the absence of synergy/antagonism.

Researchers in various fields have known for a very long time *(1, 2)* that the 'obvious' method of comparing mixture effects with simply adding component effects is wrong unless each mixture component IDER is approximately linear-no-threshold (LNT) *(3, 7, 26, 31, 32, 34)*. A replacement for simple effect additivity is therefore often needed. This paper discusses theoretical and computational aspects of the replacements.

### 1.1. Acronyms Used

There will be a number of acronyms in this paper. The main acronyms are the following, with less familiar but here often used ones, such as IDER and MIXDER, in bold-face and underlined.

- CA Chromosome Aberration(s)
- HG Harderian Gland. An organ found in many rodents
- HZE High Z and E (charge and energy) atomic nuclei, almost fully ionized
- **IDER** Individual Dose-Effect Relation, for a single agent or single mixture component
- **MIXDER** Mixture Dose-Effect Relation
- $L$=LET Linear Energy Transfer, stopping power, $LET_\infty$
- LNT Linear-No-Threshold. A straight line through the origin (dose=0, effect=0)
- **NTE** Non-Targeted Effect(s) due to inter-cellular interactions. 'Bystander' effect(s)

- ODE Ordinary Differential Equation
- **TE** Targeted Effect(s). Standard radiobiology action due to a direct hit or near miss
- WGE Whole Genome Equivalent. For CA scoring with partially painted genomes

Supplementary Information A1 reviews the mathematical notation used.

### 1.2. Mixtures and their Components

A mixed radiation field consists of N≥2 components. Each component, when acting by itself, has a dose-response relation consisting of background plus radiogenic contributions. We define the component's IDER as the radiogenic contribution. Thus by definition IDERs are zero when there is no dose above background.

### 1.3 Weaknesses of Simple Effect Additivity

One often-raised objection to the simple effect additivity synergy theory has been that, as reviewed in *(7)*, it typically violates what is called the 'sham mixture principle': mentally dividing the dose of one agent, e.g. a monoenergetic iron-ion beam, into two parts and then applying synergy theory to this sham mixture should give a baseline MIXDER equal to the agent's IDER. Fig. 1A shows a schematic, illustrative example, involving a linear-cubic IDER such as has sometimes been considered for complex chromosome aberrations, where simple effect additivity violates the sham mixture principle. The violations are symptomatic of unrealistic synergy analyses for actual mixtures. If every IDER for a mixture is convex (i.e. has positive second derivative), as in panel A, then the simple effect additivity baseline will be an unrealistic underestimate (like the dashed curve).

**Fig. 1. Simple effect additivity is not appropriate when highly curvilinear IDERs are involved.**

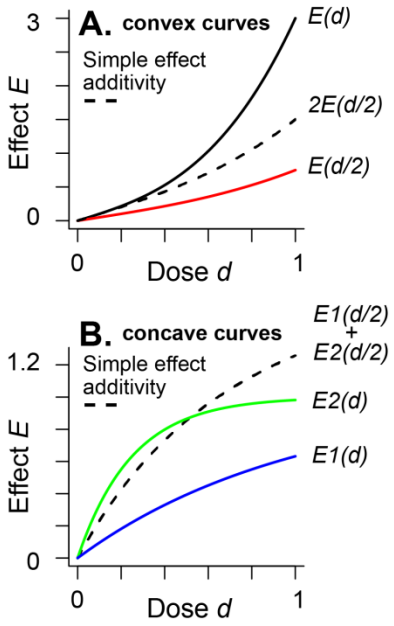


Panel **A.** Consider a hypothetical case where a 1-ion beam has IDER $E(d)=\alpha d+\omega d^3$ with $\alpha$=1 Gy$^{-1}$ and $\omega$=2 Gy$^{-3}$ (top curve). Regard the beam as a 50-50 mixture of two 1-ion beams, both of which happen to have exactly the same IDER as the original beam. Then for total mixture dose $d$, each of the two beams contributes dose $d/2$ and thus, due to the cubic term, has effect less than $E/2$ (bottom curve). Using simple effect additivity gives a baseline no-synergy/no-antagonism mixture dose-effect relation $< E$ (dashed curve) rather than the correct value $E$. Fig. 1B shows a different problem with simple effect additivity (see text).

Panel **B** in Fig. 1 shows results for hypothetical 1-ion dose response curves $E_k(d_k)=1-\exp(-\alpha_k d_k)$ with $k$=(1,2), $\alpha_1$=4 Gy$^{-1}$, and $\alpha_2$=1 Gy$^{-1}$. Instead of being approximately the average of the two IDERs the simple effect additivity baseline dose effect relation for a 50-50 mixed ion beam of the two ions (dashed curve) becomes larger than that for either ion by itself even though it is supposed to characterize absence of synergy. Similarly misleading synergy assertions arise whenever all components of a mixture have concave IDERs, i.e. IDERs with negative second derivatives, and the simple effect additivity theory is used. Such problems with simple effect additivity are well known in pharmacometrics, toxicology, evolutionary ecology and other fields of biology *(34)*. Alternatives are needed to plan and interpret mixture experiments.

### 1.4. Many Synergy Theories

In biology, there are now many different synergy theories. Some of the theories are described, reviewed and compared in *(3, 7, 9, 12, 17, 18, 20, 22, 23, 25, 26, 31, 32, 34, 38, 39)*. Generally no two of these theories are fully equivalent, though almost all give the same results for a

mixture each of whose components' IDERs is LNT. To avoid confusion, which is rife in this area, it is important to characterize carefully the particular theory used *(34)*.

This paper emphasizes one recently introduced alternative to simple effect additivity, incremental effect additivity *(39)*. 'Incremental' refers to the fact that an ordinary differential equation (ODE) is used. Intuitively speaking: incremental effect additivity deals with slopes; an IDER slope of course defines a linear relation between a sufficiently small dose increment and the corresponding effect increment *(5)*; thus by analyzing sufficiently small increments one can circumvent the curvilinearities that plague simple effect additivity estimates. For example incremental effect additivity does obey the sham mixture principle. This incremental approach has become practical because computers have become adept at solving non-linear ODE.

### 1.5. Limitations of Synergy Theories

All known synergy theories have substantial limitations. Because such limitations are sometimes soft-pedaled, we discuss most of the major ones at some length.

For example, every published alternative to simple effect additivity requires some restrictions on IDERs that limit its scope. Often monotonic increasing IDERs are explicitly required or implicitly assumed. Also, as already mentioned, synergy theory produces only a baseline MIXDER. Mixture component interactions can produce synergy or antagonism, i.e. deviations from the baseline. Mathematical manipulations of IDERs are needed to define synergy but cannot predict it *(12)*. If there is significant synergy or antagonism, biophysical insights and multiple mixture experiments or observations, not just mathematical manipulations of IDERs, are needed to characterize mixture effects *(3, 7, 26, 33, 37)*. A related limitation is that *in silico* synergy analysis becomes less and less important as fundamental biophysical understanding of mixture effects grows (Fig. 2).

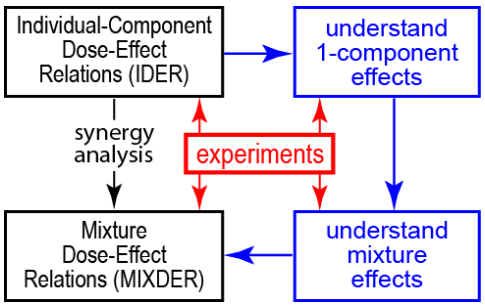


**Fig. 2. Investigating mixture effects: a long hard road or a temporary shortcut.** Eventually, but almost certainly not soon, synergy analysis of mixed radiation field effects based solely on mathematical manipulations of IDERs (leftmost downward arrow), will be replaced by biophysically-based predictions that incorporate whatever synergy or antagonism actually occurs (blue path). For the time being, optimizing synergy theory, a much simpler, faster and cheaper shortcut, is important.

### 1.6. Preview

To illustrate synergy theory, this paper calculates baseline no-synergy/no-antagonism MIXDERs for recently proposed and for illustrative hypothetical mixture experiments. We will use mixture examples, such as the mixed radiation field above low earth orbit, where some of the components are believed to induce non-targeted effects (NTE) *(21, 27, 29, 35, 36, 40, 41)*, with cells directly hit by an ion influencing nearby cells through intercellular signaling. Models of NTE action that are comparatively smooth (specifically, have continuous first and second derivatives) use IDERs very curvilinear at low doses, so our examples will often compare incremental effect additivity and simple effect additivity synergy theories.

Supplementary Information sections A1-A5 supplement the specific examples with a broader overview of current synergy analysis, emphasizing mathematical and statistical aspects relevant or potentially relevant to radiobiology. For example, Supplementary Information A5 discusses a ‘mixtures of mixtures principle’ relevant to radiobiological synergy analyses because of the fact, reviewed, e.g., in *(27, 37)*, that each individual component of a mixed radiation field is usually itself a mixture due to degradation (e.g. by self-shielding in a mouse) by the time it hits its target.

## 2. Methods

### 2.1. Customized Software

We use the open-source computer language R *(24)*, initially designed for statistical calculations but now rapidly gaining acceptance among modelers *(30)*. Our customized source codes are available at https://github.com/rainersachs/SynergyRadRes/ . Readers can freely download, use and modify them to evaluate our conclusions critically.

### 2.2. IDERs

#### *2.2.1. Some Notation*

Mixed $N$-beam irradiation with dose $d_j$ of component beam $j$ ($j$=1, …, $N$) is considered. Component IDERs are denoted $E_j(d_j)$, or sometimes $E(d)$. Sometimes biophysical parameters such as LET $L$ are used to characterize the different components and replace the label $j$, e.g. $E(d;L)$ instead of $E_j(d_j)$.

#### *2.2.2. Standard IDERs*

We define an IDER $E_j(d_j)$ as 'standard' if it obeys the following restrictions. (a) It has continuous first and second derivatives at all relevant doses including $d$=0. For example a linear IDER with threshold is not standard because at the threshold point the first derivative is discontinuous and the second derivative is infinite. (b) $E_j(d_j)$ is monotonically increasing in some half-open dose interval $[0, A_j)$.

#### *2.2.3. Calibrating Background and Radiogenic Effects Separately*

Synergy is typically considered as due to interactions among agents. Our mathematical synergy analysis applies to radiogenic effects. In calibrating $E_j(d_j)$ from data we always use only data at non-zero doses, $E_j(0)$ being 0 by definition . Background, designated by $Y_0$, is based on the zero-dose data for sham irradiated controls. $Y_0$ is needed when calibrating IDERs from data or

comparing baseline MIXDERs to data. However the main synergy calculations involve only IDERs, not background plus radiogenic, effects.

## 2.3. Synergy Theory Calculations

### *2.3.1. Notation*

Consider acute irradiation with a mixed beam of $N \geq 2$ different radiation qualities. The dose proportions $r_j$ that the different qualities contribute to total dose $d = \sum_{j=1}^{N} d_j$ obey the equations

$$d_j = r_j d; \quad r_j > 0; \quad \sum_{j=1}^{N} r_j = 1. \tag{1}$$

In our subsequent calculations $r_j$ will always, for convenience, be independent of dose. Dose independent proportions $r_j$ model one typical pattern for irradiation. The assumption of dose-independent proportions does not affect the final results. It implies that any one of the $d_j$ can be considered a control variable on essentially the same footing as the total dose $d$ since $d_j$ determines $d$, via $d=d_j/r_j$ with $r_j>0$, and thereby determines each $d_i=r_i d_j/r_j$. However we will distinguish sharply between the dose control variables $d$ and $d_j$ vs. total mixture effect considered as a control variable. In our analyses effect magnitude is sometimes used to determine $d$ and $d_j$, instead of being determined by one of them.

After parameter calibration, the IDERs $E_j(d_j)$ of all components will here be known explicit functions of dose although in general high quality numerical approximations are almost equally useful in synergy analyses.

### *2.3.2. Simple Effect Additivity S(d)*

Using the notations specified above, the baseline no-synergy/no-antagonism MIXDER of the simple effect additivity theory, denoted by $S(d)$, is:

$$S(d) = \sum_{j=1}^{N} E_j(d_j). \quad (2)$$

We shall sometimes use the notation $S(d)$ as shorthand to indicate the simple effect additivity theory is being assumed.

*2.3.3. Inverse Functions*

Inverse functions (sometimes called compositional inverse functions) are needed when using effect, rather than dose, as the independent variable. A familiar radiobiology example of inverse functions occurs when calculating the relative biological effectiveness (RBE) of two different radiations. Inverse functions play a prominent role in various synergy theories. The inverse of a monotonically increasing function undoes the action of the function. For example, for x>0, $\sqrt{x^2} = x$ so the positive square root function is the inverse of the squaring function; note that the inverse of $x^2$ is not $x^{-2}$. As another example $\exp[\ln(x)] = x$ for $x>0$, and $\ln[\exp(y)] = y$ so the functions exp and ln are inverses of each other.

*2.3.4. The Equation of Incremental Effect Additivity*

When simple effect additivity theory *S(d)* is inappropriate, incremental effect additivity theory, which replaces *S(d)* with an incremental effect additivity baseline MIXDER $I(d)$, can be useful. $I(d)$ has a number of conceptual and practical advantages over other known replacements for simple effect additivity.

A special case of $I(d)$ was defined and motivated in *(39)* under the following assumptions. Suppose we have a mixture of $N$ components with each component IDER 'standard' as defined in sub-section 2.2.2. It follows that each component IDER has a compositional inverse function $D_j$, defined for all sufficiently small non-negative effects $E$. As discussed in sub-section 2.3.3

this means $D_j(E)=d$ when $E=E(d)$. The definition was that $I(d)$ is the solution of the following initial value problem for a first order, typically non-linear, ODE:

$$dI / dd = \sum_{j=1}^{N} r_j \left[ dE_j / dd_j \right]_{d_j = D_j(I)}; \; d = 0 \Leftrightarrow I = 0, \tag{3}$$

with $r_j$=constant>0 being again the fraction of the total mixture dose contributed by the $j^{th}$ component. Supplementary Information A3.4 outlines the proof that under our assumptions there is a unique, monotonically increasing solution $I(d)$ at least for all sufficiently small non-negative values of $d$.

In Eq. (3), the square bracket with its subscript indicates the following calculations. First find the slope of the $j^{th}$ IDER curve as a function of individual dose $d_j$. Then evaluate $d_j$ using the inverse function $D_j$ with the argument of $D_j$ being the effect $I$ already present due to the influence of all the components acting jointly. Using $d_j = D_j(I)$ in Eq. (3) instead of the seemingly more natural $d_j = D_j(E_j)$ is the key assumption made. Using $d_j = D_j(E_j)$ would merely lead back to simple effect additivity $S(d)$, as proved in Supplementary Information A3.4.

Eq. (3) can be interpreted as follows. As the total mixture dose $d$ increases slightly, every individual component dose $d_j$ has a slight proportional increase since $dd_j/dd = r_j>0$. Therefore every mixture component contributes some incremental effect. The size of the incremental effect is determined by the state of the biological target, specifically by the total effect already contributed by all the components collectively (and <u>not</u> by the dose the individual component has already contributed). In this way different components appropriately track changes of slope both in their own IDER and in the other IDERs. Eq. (3) is a special case of the general equation of incremental additivity, given in Eq. (20) below, which applies when some mixture components

have non-standard IDERs. For the time being we confine attention to the special case, Eq. (3), and assume all component IDERs for a mixture are standard.

*2.3.5. Computational Implementation*

Synergy theory is applied using the IDERs with $E_j(0)=0$, and then the background $Y_0$ is added back in to the calculated baseline no-synergy/no-antagonism MIXDER for potential comparison to observed mixture results. Computing $I(d)$ for mixtures requires using a 1-dimensonal root finder within a numerical ODE integrator. Details on these calculations are available on GitHub.

## 2.4. Uncertainties in Mixture Effects

Synergy theory requires not only a way to calculate a baseline MIXDER defining no-synergy/no-antagonism but also a method of estimating uncertainties for the baseline MIXDER from mixture component IDER uncertainties. Taken together these two elements constitute a default hypothesis useful for statistical significance tests on mixture observations. Without such tests, it is sometimes unclear if an unexpectedly large or small observed result does or doesn't call for a follow-up experiment. We used Monte Carlo simulations *(14)* to calculate 95% confidence intervals (CI) for $I(d)$. Because it is known that neglecting correlations between calibrated parameters tends to overestimate how large CI are (web supplement to *(39)*), we used sampling techniques guided by variance-covariance matrices.

## 2.5. Summary of the Methods

For Results section examples, we will proceed as follows. First choose a data set on 1-ion mono-energetic radiations. Then choose IDERs that depend on several adjustable parameters. Then calibrate the adjustable parameters from the data, usually by non-linear inverse least squares weighted regression. Typical outputs for the calibration step are average values and variance-covariance matrices for the adjustable parameters. Synergy theory calculations are then carried

out, and the final results are presented in figures illustrating some specific aspects of synergy theories.

Fig. 3 summarizes these steps. Because our emphasis throughout is on illustrating different aspects of synergy theories, the early steps in the flow chart will emphasize aspects needed for the later steps, not the biological/translational implications of the data, which have all already been discussed in the references.

**Fig. 3. Flow chart for how we present examples.**

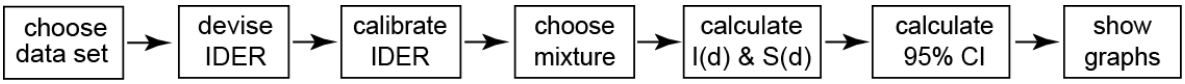

## 3. Results

We give examples which, taken together, give an overview of radiobiologically relevant synergy theory. Each example has a data set, IDERs, and mixtures (Fig. 3); the mixtures are specified by their components and the components' fraction $r_j d$ of the total mixture dose $d$. The main results are presented as IDER and baseline MIXDER graphs. The emphasis is on situations where there is evidence that NTE are important, so that standard IDERs highly curvilinear at very low doses are needed.

### 3.1. Chromosome Aberration (CA) Examples

#### *3.1.1. Data*

Two recent papers, *(29)* and *(36)* include data on Whole Genome Equivalent (WGE) simple chromosome aberrations induced by acute *in vitro* exposure, at Brookhaven NASA Space Radiation Laboratory (NSRL), of human cell line 82-6 fibroblasts to the 1-ion beams shown in Table 1.

| param | **ion** | $^{16}$**O** | $^{28}$**Si** | $^{48}$**Ti** | $^{56}$**Fe** | | |
|---|---|---|---|---|---|---|---|
| $Z$ [a] | | 8 | 14 | 22 | 26 | | |
| $E/u$ (MeV) [b] | | 55 | 170 | 600 | 600 | 450 | 300 |
| $\beta^*$ [c] | | 0.33 | 0.53 | 0.79 | 0.79 | 0.74 | 0.65 |
| $L$ (keV/μm) [d] | | 75 | 100 | 125 | 175 | 195 | 240 |
| $Z_{eff}^2/\beta^{*2}$ [e] | | 595 | 690 | 770 | 1075 | 1245 | 1585 |
| *dmax* (Gy) [f] | | 0.4 | 1.2 | 0.6 | 0.8 | 0.4 | 0.8 |

**Table 1. Ion Parameters.**

[a] $Z$ is atomic number. [b] $E/u$ is kinetic energy per atomic mass unit. [c] $\beta^*$ is ion speed relative to the speed of light. [d] $L$ is *LET*. [e] $Z_{eff}$ is the effective ion charge, only very slightly less than $Z$ for these high-speed ions. [f] *dmax* is the maximum dose for that ion in the data set.

The ions are thus high-charge, high-energy (HZE) and high LET. The data is for experiments where the only shielding was from matter unavoidably in the beam, with no extra shielding intentionally added. Evidence that at very low doses NTE produce CA in these fibroblasts was given in *(36)*.

Similar 82-6 fibroblast experiments at NSRL are ongoing. These sometimes use additional kinds of ions (such as protons), or, importantly for our purposes, use ion mixtures. The results have not yet been published and are not considered in this paper. However, we have aimed at providing a suitable framework for systematic synergy analysis of the ongoing mixture experiments, using information on their component's IDERs from *(29, 36)*, and/or from subsequent 1-ion experiments.

*3.1.2. Small Background CA Frequency*

In synergy calculations, background effects are first subtracted out, as described in the Methods section. For the HZE experiments in *(29)* there were a total of 7401 zero-dose, control cells in the experiments for 5 HZE ions, and a total of 6 whole genome equivalent simple CA scored (M. Hada, private communication). Adding in 1008 control cells for Ti ion experiments with no CA scored (web supplement to *(36)*) gives an estimate of background effect as $Y_0 = 6/8409 = 7 \cdot 10^{-4}$ per cell. This number is so small that it did not significantly influence any of our results.

*3.1.3 Preliminary Comments*

The next step toward synergy analysis is to choose IDERs (Fig. 3). In *(36)* various IDER models, based on modifications of Katz' amorphous track structure approach *(6, 15, 19, 28)* were used by Hada, Cucinotta and coworkers to analyze the data; two of their models, reviewed in Supplementary Information A2, incorporate both TE and NTE. We modified these two models to obtain our IDERs. To illustrate synergy analysis we needed IDERs that are monotonic increasing

and have finite slope at all relevant doses including $d$=0. Additional criteria we used included the following: keeping the number of adjustable parameters to a minimum; using only adjustable parameters that differ significantly from zero; having Akaike and Bayesian information criteria scores that compare favorably with scores for the two relevant models in *(36)*; and otherwise modifying these models as little as possible.

General properties of our resulting IDERs after calibration are shown in Fig. 4. At very low doses, where NTE effects putatively dominate, the IDERs rise with a very large but finite slope and have marked curvilinearity, specifically concavity.

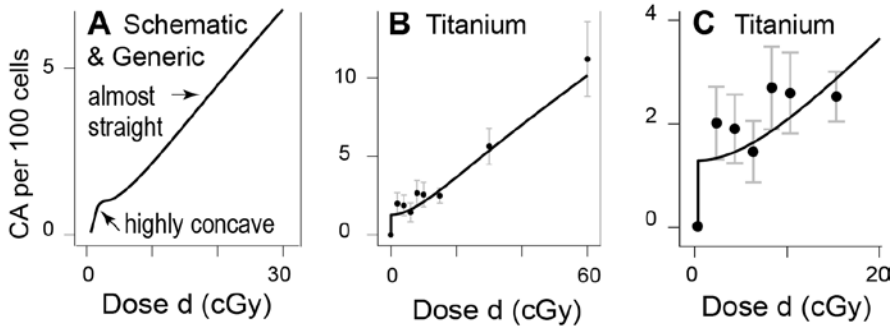


**Fig. 4. IDER shape.** The vertical axis is WGE simple aberrations per 100 cells. Panel A shows qualitative features of the IDERs. To emphasize that there is a finite, smoothly changing slope even near $d$=0, the steep rise and marked curvilinearity at very low doses has been visually understated in the schematic panel, panel A. Panels B and C are to scale. The curves, actually smooth, incorrectly suggest an infinite slope followed by a kink at $d$=0. The steep rise at low doses is inferred indirectly, not observed directly: effects observed at somewhat larger doses (~ 1 cGy or more) are higher than a LNT model can readily account for.

At doses >0.1 Gy TE putatively dominate and the slope is almost constant, putatively corresponding to high LET 1-track action dominating at doses between 5 and 50 cGy. The published data for the other 5 ions in Table 2 are reviewed in Supplementary Information A2.

We will use the same symbols for our adjustable IDER parameters as were used for corresponding parameters in *(36)* in corresponding equations. The correspondences are approximate, not exact.

*3.1.4 Adjustable Parameters Used*

Our IDERs use 4 adjustable parameters $\eta_0$, $\eta_1$, $\sigma_0$, and $\kappa$. Table 2 shows their units and their values after calibration. For example in the IDERs one term will be of the form $\exp(-\eta_1 L)$. The units of LET $L$ are keV/μm and an exponential must have a dimensionless argument, so $\eta_1$ has dimensions μm(keV)$^{-1}$. Table 2 also repeats the value for the background frequency. All four IDER parameters were significantly different from 0 at the $p< 0.1$ level, three at the $p<0.01$ level, and two at the most stringent level usually considered, $p<0.001$. These $p$ levels were a pleasant surprise.

**Table 2. Calibrated Parameters**

| | Units | Value | $p$ | Comments |
|---|---|---|---|---|
| $Y_0$ | dimensionless | 7e-5 [a] | NA | Background. See sub-section 3.1.2 |
| $\eta_0$ | dimensionless | 1.5e-4±2.2e-5 | 2e-08 | Both parameters help specify how NTE magnitude depends on LET $L$ |
| $\eta_1$ | μm(keV)$^{-1}$ | 3.5e-3±9.0e-4 | 3e-4 | |
| $\sigma_0$ | μm$^2$ | 4.2±1.4 | 4e-3 | Both parameters help specify TE slope as a function of $d$, $L$, and $Z_{eff}^2/\beta^{*2}$ |
| κ | dimensionless | 469±247 | 6e-2 | |

[a]Powers of 10 are indicated by 'e', for example 3.5e-3=0.0035.
[b]Standard errors are indicated by ± .

*3.1.6. IDERs Used: Equations*

Before carrying out synergy analysis we must devise and calibrate IDERs. We will use 6 equations to specify the IDERs. The first is

(3.1.1) $$E_{total} = Y_0 + E(d; L, Z_{eff} / \beta^*) = Y_0 + E_{TE}(d; L, Z_{eff} / \beta^*) + E_{NTE}(d; L). \quad (4)$$

Here $E_{total}$ is for background + radiogenic effect. $E(d;L,Z_{eff}/\beta^*)$ is an IDER, 0 at $d=0$. $E_{TE}$ and $E_{NTE}$ respectively indicate additive contributions modeling TE or NTE.

In $E_{TE}(d;L,,Z_{eff}/\beta^*)$, the dose dependence is written in terms of ion flux $F$ (i.e. particle tracks per unit area) and a hit number $H$ proportional to $F$, which are given by

$$F = 6.242(d/L); \qquad H = FA; \qquad A = 162\ \mu\text{m}^2. \tag{5}$$

Here the factor 6.242 applies when areas are given in $\mu$m$^2$ and dose is given in Gy. The value for $A$ was, as described in *(29, 36)*, determined by measurements of the beam-perpendicular cross sectional area of 82-6 fibroblast nuclei. $H$ is the total number of ion track cores that intersect an 82-6 fibroblast nucleus at dose $d$. Our version of the TE contribution is

$$E_{TE}(d;L,Z_{eff}/\beta^*) = \sigma F\left[1-\exp(-H)\right], \tag{6}$$

where the dose-independent quantity σ is, using the notation of Tables 1 and 2,

$$\sigma = \sigma_0 P + \frac{\alpha_\gamma L}{6.242}(1-P); \quad P = \left[1-\exp\left(-\frac{Z_{eff}^2}{\kappa\beta^{*2}}\right)\right]^2. \tag{7}$$

In Eq. (7): we chose the parameter $m$ in the corresponding equation in *(36)* as $m$=2 on the biophysical grounds that it takes 2 DNA double strand breaks to make one simple CA; $\alpha_\lambda$ is the linear coefficient of the linear-quadratic fit to the gamma-ray dose-effect relationship for WGE simple CA per cell. A separate calculation in *(29, 36)* gave $\alpha_\lambda$ = 0.041±0.0051 Gy$^{-1}$ and we here use this value throughout. Table 2 gives the values of $\sigma_0$, and $\kappa$. For $\kappa$ >0, 1>$P$>0.

In Eq. (4)), combining Eqs. (5)-(7) specifies the TE term $E_{TE}(d;L)$ so we only need to specify the NTE contribution to complete the characterization of our IDERs, as follows.

$$E_{NTE}(d;L) = \eta(L)\left[1-\exp(-d/d_0)\right]. \tag{8}$$

Here, much as in *(36)*,

$$\eta(L) = \eta_0 L \exp(-\eta_1 L) \quad (9)$$

specifies an LET-dependent saturation level for NTE at doses larger than 1 mGy. The saturation level rises linearly for small LET, reaches a maximum at $L=(1/\eta_1)$, and then decreases. For the average value of the adjustable parameter $\eta_1$ in Table 2, the maximum occurs at $L$ = 230 keV/μm.

In Eq. (8) $d_0$ is a nominal, very small dose. The data considered are not informative about any details at very low doses < 1 mGy. They do suggest NTE which lead to a large <u>average</u> positive slope at very low doses, whose cumulative influence builds up a CA frequency $E_{NTE}$ sufficiently large to be detectable above background and noise at doses ≥ 0.01 Gy. To take into account NTE dose dependence in a way consistent with the concavity found in mechanistic models for NTE for other endpoints *(16)* we used the factor [1-exp(-$d/d_0$)] and used $d_0$= $10^{-5}$ Gy. Numerical explorations show that the final results are insensitive to $d_0$ as long as $d_0 \ll 10$ mGy.

*3.1.6. Summary of IDER Equations*

Rearranging Eqs. (4)-(9) to show more concisely the dependence on all four adjustable parameters (i.e. $\eta_0$, $\eta_1$, $\sigma_0$, and $\kappa$), our IDERs $E(d)$ are

$$E(d) = \eta_0 L \exp(-\eta_1 L)\left[1 - \exp(-d / d_0)\right] + \left[\sigma_0 P + \alpha_\gamma L(1-P) / 6.242\right] F\left[1 - \exp(-H)\right], \quad (10)$$

where $\alpha_\lambda$ = 0.041±0.0051 $Gy^{-1}$, $d_0$=$10^{-5}$ Gy, and

$$P = \left[1 - \exp\left(-\kappa^{-1} Z_{eff}^2 \beta^{*-2}\right)\right]^2. \quad (11)$$

The biophysical parameters such as LET $L$ are those in Table 2. In Eq. (10), the first term in the sum is for NTE; the second term is for TE. As shown in Eq. (5), $F$ is the particle flux, proportional to $d/L$, and hit number $H$ is proportional to $F$. Thus when $H$ becomes so large that exp(-$H$) is negligible, the TE term has constant slope (Fig. 4).

*3.1.7 IDER Calibration*

The IDERs were calibrated by using non-linear least squares inverse variance weighted regression with the Levenberg-Marquand algorithm to determine the four adjustable parameters from combined data of all six ions at all non-zero doses. The auxiliary parameter $\alpha_\lambda$ and the background value $Y_0$ were held fixed at their central values during the calibration. The results for the four adjustable parameters were shown above, in Table 2.

The regression also determined a variance-covariance matrix, shown in Table 3, which we will use during synergy analyses in calculating 95% CI for the baseline incremental effect additivity MIXDER $I(d)$.

**Table 3. Variance-Covariance Matrix**

| | $\eta_0$ | $\eta_1$ ($\mu$m/keV) | $\sigma_0$ ($\mu m^2$) | $\kappa$ |
|---|---|---|---|---|
| $\eta_0$ | 4.80e-10 [a] | 1.94e-08 | 9.10e-06 | 2.08e-03 |
| $\eta_1$ | 1.94e-08 | 8.17e-07 | 5.33e-04 | 1.05e-01 |
| $\sigma_0$ | 9.10e-06 | 5.33e-04 | 1.87 | 3.13e+02 |
| $\kappa$ | 2.08e-03 | 1.05e-01 | 3.13e+02 | 6.10e+04 |

[a] The 'e' entries mean powers of 10, e.g. 4.8e-10 = $4.8 \times 10^{-10}$

The corresponding parameter correlation matrix is shown in Table 4. In this case, all correlations happen to be positive. For example, the strong positive correlation between $\eta_0$ and $\eta_1$ was expected intuitively because the only way $\eta_0$ and $\eta_1$ appear in the IDERs is via the combination $\eta_0 \exp(-\eta_1 L)$. Thus this combination is anchored in the data and its fluctuations will tend to be small. If $\eta_0$ is above (respectively below) average then holding the combination constant requires an above (respectively below) average value of $\eta_1$, i.e. anchoring the combination in the data leads to positive correlations.

**Table 4. Pairwise Parameter Correlations.**

| | $\eta_0$ | $\eta_1$ | $\sigma_0$ | $\kappa$ |
|---|---|---|---|---|
| $\eta_0$ | 1 | 0.98 | 0.30 | 0.38 |

| | | | | |
|---|---|---|---|---|
| $\eta_1$ | 0.98 | 1 | 0.43 | 0.47 |
| $\sigma_0$ | 0.30 | 0.43 | 1 | 0.93 |
| $\kappa$ | 0.38 | 0.47 | 0.93 | 1 |

*3.1.8. Synergy Analyses for 2-ion and 6-ion mixtures*

With our IDERs calibrated, the next step was to carry out synergy analyses. Sub-section 3.1.8 works entirely with the average values shown in Table 2. Discussing uncertainties in MIXDERs is postponed till the next sub-section.

Systematic synergy analysis requires known IDERs as a starting point. The only IDERs (or data) for this data set are for primary beams (upstream of any incidental matter in front of the biological target) consisting of a single HZE ion with $Z \geq 8$, so our mixture examples perforce involve only such HZE components. We believe such mixtures are in any case more interesting than mixtures where most of the dose in the primary beam is contributed by low LET protons and alpha particles. The HZE part of the GCR spectrum has caused much concern about astronaut exposures during prolonged periods above low earth orbit, and synergy between specific HZE components would compound the worries.

Fig. 5 shows, for a 50-50 Si-Fe mixture, prototypical results contrasting our preferred no-synergy/no-antagonism baseline MIXDER $I(d)$ with simple effect additivity $S(d)$. It is seen in panel B that the NTE part of $S(d)$, which dominates the MIXDER at very low doses, shows saturation at about the sum of the two IDER NTE contributions, rather than their average. This is merely the same artificial result shown in Fig. 1B: $S(d)$ tends to be an unrealistic over-estimate whenever all mixture components are highly concave. To our knowledge, there are no known mechanistic reasons why NTE effects in a mixture should saturate at effect higher than the height of the NTE part of either component acting by itself. In contrast, the NTE part of $I(d)$ saturates at about the larger of the two. The next figure will show that for a mixture of many HZE ions,

corresponding patterns lead to strong differences between simple and incremental effect additivity baselines even at doses ~ 50 cGy.

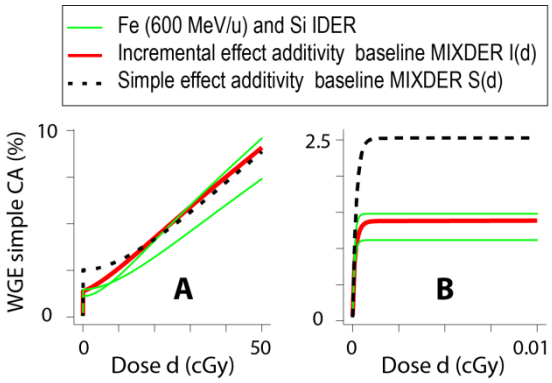


**Fig. 5. Synergy Analysis for a Si-Fe Mixed Beam**. The figure shows baseline curves (black dashed and red solid) for a mixture of Si (170 MeV/u, $L$=100 keV/μm) and Fe (600 MeV/u, $L$=175 keV/μm) with proportions $r_1$ = 0.5 = $r_2$. Panel A shows the overall curves up to mixture dose 0.5 Gy. Panel B zooms in by a factor of 5,000 to show details about the mathematical model at doses too small for CA data to be available.

Green lines show the IDER curves that would result if the entire dose were contributed by one of the two ion beams instead of being split 50-50. Here the Fe IDER is the one that is lower at 50 cGy but higher at very low doses.

Details of the calculations that produced Fig. 5 are encapsulated in the customized open-source programs that can be freely downloaded from GitHub.

The choice $r_1$=0.5 (so that $r_2$=0.5 also) in the mixture of Fig. 5 was arbitrary. If one wants to check experimentally whether mixing the two beams ever leads to statistically significant synergy or antagonism one would have to calculate a few more cases, say $r_1$=0.2, $r_2$=0.8 and $r_1$=0.8, $r_2$=0.2. When we set out to give examples involving N>2 ions we were unpleasantly surprised to find that, due to the many possible choices of the $r_j$, the number of possible examples grows very rapidly as N increases. Worse, there is no systematic way to choose any particular example. Thus the example given next is not chosen in any systematic way, and apparently could not be chosen systematically without giving a very large number of examples.

Fig. 6 gives another example of a mixture. It illustrates the fact that $S(d)$ for a mixture of many ions which individually can produce significant NTE gives an unreasonable baseline

MIXDER even at doses large enough for data to be available. In Fig. 6 it specifies that, at low doses, effects much larger than any component would produce if acting by itself with the total mixture dose are ostensibly not synergistic. Calculations not shown indicate that if a mixture consists of many more than 6 HZE ions the difference at low doses between $S(d)$ and all the component IDERs becomes much larger, with $S(d)$ specifying absurdly high effects as defining absence of synergy. In contrast, $I(d)$ specifies saturation near the top of individual component saturation heights and tends to remain nested within the component IDERs.

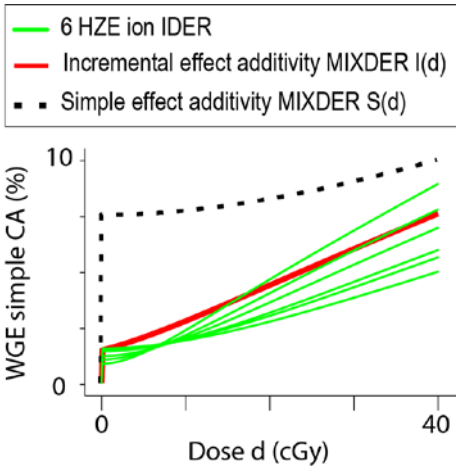


**Fig. 6.** The figure shows results for a mixture of all 6 ions in Table 1, with each contributing 1/6 of the total dose $d$. The green lines show the six component IDERs. The IDER curve heights at low doses are in the same order as the LETs; e.g. the highest green curve is for Fe ions with energy 300 MeV/u and LET 240 keV/$\mu$m. Above 10 cGy the order is reversed.

As in Fig. 5, $I(d)$ specifies saturation of NTE effects at the height of the component IDER with the largest low dose NTE height.

*3.1.9. 95% CI for $I(d)$*

Our calculations include finding 95% CI for $I(d)$ (Fig. 3). We used Monte Carlo simulations to calculate 95% CI for the incremental effect additivity baseline no-synergy/no-antagonism MIXDER of the two-ion mixture of Fig. 5, taking into account parameter correlations. We had to make ad-hoc adjustments for cases where $\kappa$ or $\sigma_0$ were not > 0. This occurred about 3% of the time and did not affect the CI significantly. Details are again encapsulated in the customized open-source codes that can be downloaded from GitHub.

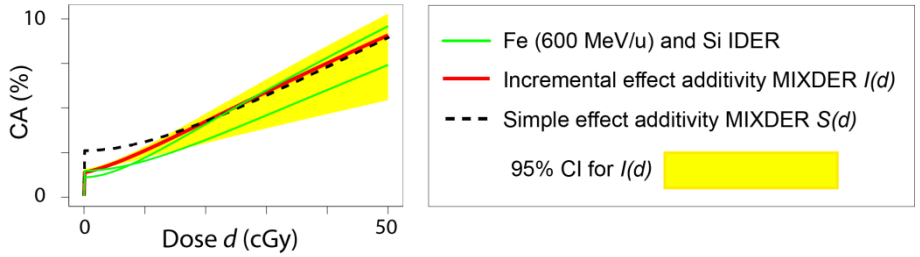


**Fig. 7. 95% CI in the 2-ion mixture.** It is seen that for a 2-ion mixture the two baseline no-synergy/no-antagonism dose effect relations have statistically significant differences only for doses less than about 0.05 Gy.

We also calculated 95% CI for the 6-ion mixture of Fig. 6. In order to estimate how much neglecting parameter correlations overestimates the 95% CI, we compared two alternative calculations. Fig. 8 shows the results.

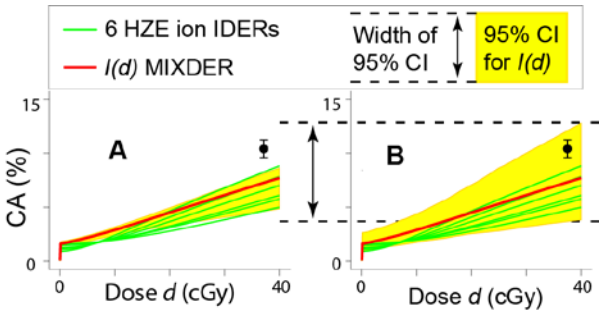


**Fig. 8. CI for *I*(*d*).** Panel A shows the calculated 95% CI if parameter correlations are taken into account appropriately. Panel B shows calculated 95% CI if the correlations are unrealistically neglected.

At *d*=40 cGy, panel B overestimates the 95% CI in panel A by a factor of ~ 2.35. The black circle with error bars shows a possible data point in a mixture experiment.

Of note in figure 8 is that a mixture experiment which leads to the black circle with error bars would be, as is clear from panel A, statistically significant evidence of synergy. Using panel B would misinterpret the same measurement as merely suggestive, not statistically significant. Thus taking parameter correlations into account, though often neglected, is important when interpreting mixture experiments.

*3.1.10. Summary*

We used CA models to illustrate various aspects of mathematical synergy analyses. Assuming non-targeted effects are important, *I*(*d*) gives a markedly different, more reasonable, no-

synergy/no-antagonism baseline than does $S(d)$ when mixtures of many HZE are considered. There is a bewildering number of potentially inequivalent mixtures whenever more than a few ions are involved. As yet unpublished data on ongoing experiments will be a test of our IDERs, as well as providing some mixture data to compare with $I(d)$.

### 3.2. An Example Using Murine Harderian Gland (HG) Tumorigenesis Data

Our second example uses a famous data set. It further illustrates marked IDER curvilinearity. It will again be presented in the order indicated by Fig. 3: first the data set, then IDERs, then MIXDERs. From here on, we will graph only curves using average values for the adjustable parameters, not 95% CI for $I(d)$, which are adequately exemplified above.

#### *3.2.1. Accumulating Data*

Many rodents have Harderian glands, an epithelial tissue. An extensive set of experimental observations is available on the fraction of female B6CF1/Anl mice that develop at least one radiogenic HG tumor after exposure at various doses to various 1-ion HZE beams *(4, 10, 11, 13, 35)*. This fraction, the tumor prevalence, is by definition $\leq 1$. The HZE ions' parameter ranges are: atomic charge $8 \leq Z \leq 57$; approximate LET $20 \leq L\ (keV/\mu m) \leq 950$; approximate speed relative to speed of light $0.61 \leq \beta^* \leq 0.81$. All the relevant data in the references is reviewed in customized open-source software freely downloadable from GitHub. Additional data in the same data set -- on fast, low LET protons and alpha particles -- will be discussed in sub-section 3.3 below. Unpublished data from ongoing experiments includes other ions plus some mixed-beam exposures; these as yet unpublished data will not be used in this article.

#### *3.2.2. Adjustable Parameters Used*

Our HZE IDERs use 3 adjustable parameters $a_1$, $a_2$, and $\eta$ (Table 5). As in Table 2 we also show the parameter values after they have been calibrated and the value for the background

frequency. The background frequency was taken from recent modeling of the same data *(35, 41)* without further calculations on our part, as the emphasis here will again be on using IDERs in synergy analyses rather than biophysically interpreting IDERs.

**Table 5. Calibrated Parameters**

| | Units | Value (%) | *p* | Comments |
|---|---|---|---|---|
| $Y_0$ | dimensionless | 2.7 | - | Background. |
| $a_1$ | μm(keV)$^{-1}$ | 8e-1±1e-1 [a] | 3e-8 | Both parameters help specify how TE slope depends on LET *L* |
| $a_2$ | μm(keV)$^{-1}$ | 3.4e-3±4e-4 | 7e-9 | |
| $\eta$ | dimensionless | 5±1.4 | 2e-6 | NTE height |

[a]Powers of 10 are indicated by 'e', for example 8e-1=0.8. standard errors are indicated by ± . Thus all three IDER parameters were significantly different from 0 ($p$<1e-5). The most recent published analysis of the same data *(41)* used NTE IDER with four adjustable parameters, 3 having p-values <$10^{-4}$, but one having $p$=0.4.

*3.2.3. IDERs Used*

The IDERs we use here for the HZE data modify some of the tumor prevalence models in *(35)* and *(41)*; they are NTE models, i.e. assume both TE and NTE are significant. For all doses they are less than 1, the maximum possible value since prevalence refers to animals with at least one tumor.

The starting point for our models is a clever hazard function equation suggested by Cucinotta and coworkers, e.g. *(41)*:

$$E(d) = 1 - \exp[-H(d)]. \quad (12)$$

Here $E(d)$ is the IDER and $H(d)$ is a non-negative hazard function, which we shall use to define $E(d)$. Eq. (12) is an important improvement over earlier models of the HZE HG data because it

incorporates the limitation that $E(d) \leq 1$ without needing to add any extra adjustable parameters. Specifically, we shall use hazard functions which are themselves smooth, monotonically increasing IDERs. Then $E(d)$ in Eq. (12) is automatically a smooth monotonically increasing IDER: $H$, being an IDER, is zero at dose zero by definition and then Eq. 12 implies $E(0)=0$.

However, our HZE models do not adopt the Katz type approach of *(41)*. We found HZE models with fewer adjustable parameters and improved *p*-values. And we felt that when applied to NTE models the approach in *(41)* becomes harder to motivate, e.g. as regards effects of delta rays on NTE and as regards the way in which cell killing terms appear in the equations.

Specifically, we used for $H$ an LET dependent TE term linear-no-threshold in dose that involves two of the adjustable parameters in Table 5. We added an LET-independent NTE term involving our third adjustable parameter, $\eta$, to get the following equation.

$$H(d;L) = a_1 L \exp\left[-a_2 L\right] d + \eta\left[1 - \exp(-d / d_0\right]. \quad (13)$$

In this equation, $d_0$ is again a nominal, very small dose having all of the properties given in the paragraph below Eqs. (8) and (9). In particular, all our final results are independent of $d_0$ provided $d_0 < 10^{-5}$ Gy.

After calibration, our IDERs were considered applicable to all heavy ions in the Z, LET, and energy ranges covered by the data, even to 1-ion beams not in the data set. The relevant ranges were $8 \leq Z \leq 43$, $25 \leq L$ (keV/$\mu$m)$\leq 950$, $360 \leq E$ (MeV/u)$\leq 1000$.

*3.2.4. Results*

Fig. 9 shows an example of the results. Simple effect additivity $S(d)$ again unrealistically specifies that a mixture effect larger than that of any component defines absence of synergy and antagonism. Similar calculations show that if more than about 12 HZE ions are involved $S(d)$ makes the absurd claim that absence of synergy or antagonism at 0.5 Gy means the fraction of

mice that have at least one tumor is greater than 1. In contrast $I(d)$ in Fig. 9 is close to the average of the four IDERs at all doses larger than the nominal value of $10^{-5}$ Gy.

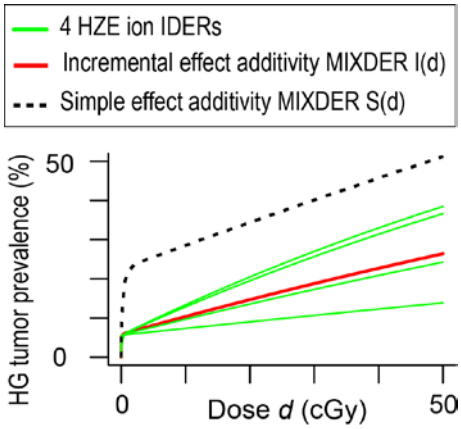


**Fig. 9. A 4-ion Mixture.** The figure shows results for ions of respective LETs (bottom to top) L=25, 70, 190, and 250 keV/$\mu$m. Each ion contributes ¼ of the total mixture dose *d*.

## 3.3. An Example of a Common Difficulty in Synergy Analysis and its Remedy.

### *3.3.1. Data*

In addition to the high LET HZE data analyzed in sub-section 3.2, the data set in *(35)* has results for fast light ions, specifically protons and alpha particles with speed roughly half the speed of light and low LETs (~0.4 to ~1.6 keV/μm). Eyeballing graphs of the data in *(35)* and other papers on the same data suggests NTE may be negligible for fast light ions. It also suggests the HG prevalence induced by the fast light ions levels off at a value less than 1; in fact some earlier models have the prevalence decreasing at large doses, although in our opinion the visual evidence also allows a plateau. This prevalence limit means that synergy analyses of a mixed beam containing both HZE ions and fast light ions encounters a difficulty that also arises for some other data sets. We now illustrate the difficulty and how it can be solved.

### *3.3.2. IDERs Used*

We will use a ‘toy’ (i.e. hypothetical) IDER for the fast light ions. It has an analytical form so simple that the contribution of the fast light ions to the baseline MIXDER slope can be computed

analytically. Its parameters are chosen so that resulting IDER and MIXDER curves show the basic patterns of interest in a visually vivid way. Actual fast light ion IDERs calibrated with the actual HG data will be discussed elsewhere. The toy IDER is

$$E(d) = M[1 - \exp(-\lambda d)], \tag{14}$$

where $M$ =0.28 and $\lambda$=0.78 $Gy^{-1}$. $M$ is the limiting value for large doses and $M\lambda$ is the slope at the origin.

The IDER is smooth, monotonically increasing, and 0 at 0 dose; calibrating $M$ quantifies the prevalence value, and thereby also the dose, at which the IDER levels off (or, in some models, even begins to decrease). When $E(d)$ obeys Eq. (14) the slope function $dE/dd$ can be expressed explicitly as a function of $E$ without using the inverse function $d=D(E)$ in an intermediate step, thereby simplifying the next few equations and allowing them to be an atypically simple illustration of an important general point. The slope is calculated as

$$dE / dd = \lambda M \exp(-\lambda d) = \lambda M[1 - (E / M] = \lambda(M - E). \tag{15}$$

Thus Eq. (14) implies

$$\text{A.}\quad dE / dd = \lambda(M - E);\ \text{and B.}\quad E(d = 0) = 0. \tag{16}$$

Conversely, Eq. (16) is an ODE initial value problem that has a unique solution. Integrating Eq. (16A), $dE/dd = \lambda(M-E)$, implies that for $E<M$ there is a constant of integration such that

$$-\lambda d = \ln(M - E) + cons. \tag{17}$$

The initial value (16B) then implies the integration constant is $-M$ and using the fact that exp and ln are inverses of each other leads directly back to Eq. (14).Thus as far as IDERs are concerned, Eqs. (14) and (16) are completely equivalent.

However, for analyzing a mixture of a light ion with an HZE, using Eq. (16) has a surprising advantage. What we need for calculating a baseline MIXDER with the equation of incremental

effect additivity, Eq. (3), is not $E(d)$ but the slope $dE/dd$ as a function of $E$; replacing $E$ by the total effect, say $I$, due to all the mixture components we then get the contribution of $E(d)$ to the mixture slope. Thus if $r$ is the fraction of mixture dose supplied by light ions, given $dE/dd = \lambda(M-E)$ we can use $r\lambda(M-I)$ as the slope contribution, even at doses so large that the HZE components in the mixture have driven $I$ above $M$ and the light ion contribution to the MIXDER slope is negative. In other words, with $E_1$ denoting the HZE IDER, we can replace Eq. (3) by

$$dI / dd = r_1\left[dE_1 / dd_1\right]_{d_1 = D_1(I)} + r_2\lambda(M - I); \quad d = 0 \Leftrightarrow I = 0. \tag{18}$$

One intuitive motivation behind Eq. (18) is that, as discussed in motivating Eq. (3), effect $I$ is a system variable, a property of the biological target, rather than being, like $d$, merely externally imposed. So $I(d)$ can supply information, in this case $r_2\lambda(M-I)$, which can help determine its own incremental changes.

An example which illustrates Eq. (18) is given in Fig. 10. In each panel the upper green curve is the IDER for a HZE mixture component that has LET 195 keV/μm. The lower green curve is the IDER for fast light ions, e.g. protons. Results for mixtures with two different dose-proportions are shown in the two panels. Eq. (18) was used to calculate baseline MIXDERs (red curves). As can be proved by the using the qualitative theory of ODE *(8)*, MIXDERs level off at an effect between $M$ and 1 where the tendency of the light ions to pull the MIXDERs down to $M$ just balances the tendency of the HZE component to pull them up to 1.

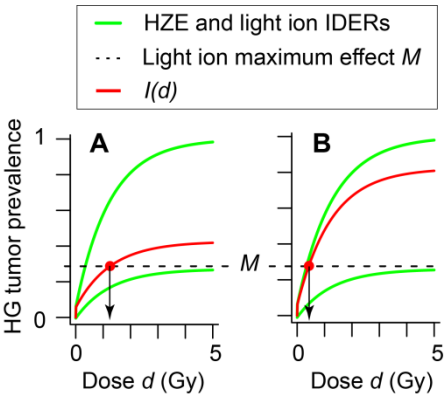


**Fig. 10. Mixtures of an HZE ion and a Light Ion.**

In panel A protons contribute $r_1$ = 80% of the mixture dose; in panel B they contribute only $r_1$ = 25%. It is seen that $I(d)$ given by Eq. (3.4.3) is well defined even for effects greater than $M$. The cutoff doses corresponding to $M$ are shown by the downward arrows. It is seen that at dose fraction 80% the protons pull the

MIXDER down close to *M* at large doses. At dose fraction 25% they can only pull it down to somewhat less than 1.

Eq. (3) and Eq. (18) give identical curves as long as the baseline MIXDER effect is less than *M*. The key point is that when the baseline MIXDER effect calculated by Eq. (18) reaches *M* (red dots) the incremental effect additivity Eq. (3) contains an undefined inverse function for the light ion so it cannot be used to calculate MIXDERs beyond the corresponding doses. This difficulty is rather similar to, though not the same as, the well-known problems [reviewed in *(42)*] that occur in trying to compute RBEs when a high LET radiation can produce effects larger than any effect the low LET reference radiation can produce.

In Fig.10, cutoff doses are about 1.2 Gy in panel A and < 0.5 Gy in panel B. Typical low-dose NASA mixture experiments do not go as high as 1.2 Gy, but a cutoff at < 0.5 Gy would be an unduly strong limitation, circumvented by using Eq. (18) instead of Eq. (3).

### 3.4. The General Equation of Incremental Effect Additivity.

Generalizing the results of the previous sub-section, consider IDERs given by

$$dE / dd = F(E); \quad E = 0 \text{ when } d = 0, \tag{19}$$

with the slope function $F(E)$ sufficiently well behaved that there is one and only one solution for all sufficiently small non-negative doses. Consider a mixture consisting of $N \geq 0$ agents whose IDERs are in the form $E_j(d_j)$ together with $K \geq 0$ agents whose IDERs are defined by Eq. (19), where $N+K \geq 2$. Let $r_1, r_2, ..., r_{N+K}$ be the corresponding proportions. Then the general equation of incremental effect additivity for $I(d)$ is:

$$dI / dd = \sum_{j=1}^{N} r_j \left[ dE_j / dd_j \right]_{d_j = D_j(I)} + \sum_{j=N+1}^{N+K} r_j F_j(I); \quad d = 0 \Leftrightarrow I = 0. \tag{20}$$

Supplementary Information A5 analyzes the mathematical properties of this equation in detail and, importantly, shows that it is often applicable even when the restriction that all IDERs be monotonic in the same direction does not hold.

### 3.5. Summary of Results

To illustrate the aspects of synergy theory likely to be most important in radiobiology we gave results exemplifying the following: the importance of having high-quality IDERs available; the use of alternatives, such as incremental effect additivity $I(d)$, to simple effect additivity $S(d)$ when IDER curvilinearity requires an alternative; calculation of baseline MIXDER 95% CI taking into account correlations between IDER adjustable parameters; and the extraordinarily rapid increase in the number of possible mixtures needed to determine synergy patterns for $N$-component mixtures as $N$ increases.

## 4. Discussion

### 4.1 Synergy Theory

For the foreseeable future radiobiologists studying mixed radiation field effects will almost inevitably emphasize possible synergy and antagonism among the different radiation qualities in the mixture. Therefore trying to find a systematic quantification of synergy, general enough to cover most cases of radiobiological interest and precise enough to enable credible estimates of statistical significance, is worthwhile. But it is not easy.

One main problem is the following. The common belief that synergy can always be defined as an effect greater than the simple effect additivity baseline MIXDER $S(d)$ is wrong. $S(d)$ can almost always be calculated, but in some important cases is clearly inappropriate. There are a number of published alternatives which seem appropriate whenever they can be calculated, but are not well defined unless all IDERs in a mixture are monotonic in the same direction. The monotonicity requirement restricts their scope unduly.

Among the alternatives to $S(d)$, the incremental effect additivity baseline MIXDER $I(d)$ seems preferable. We have here illustrated it with detailed examples of mixtures of ions in the GCR spectrum, since more experimental information on such mixtures will soon become available.

### 4.2. Summary

- Synergy theory will continue to be used to plan experiments involving mixed radiation fields and interpret the results of such experiments. It can and should include calculations that give confidence intervals based on variance-covariance matrices.
- If non-targeted effects are important the simple effect additivity no-synergy/no-antagonism baseline MIXDERs should be ignored or used only cautiously.
- Incremental effect additivity theory is in our opinion the preferred replacement for simple effect additivity theory.
- When individual dose-effect relations for components of a mixture are all monotonically increasing there are many other synergy theories that have been developed over many years in many different fields of biology to supplement or replace simple effect additivity.
- In any case, all synergy theories have more limitations than is generally realized.
- Whether mixing GCR components ever leads to statistically significant synergy for animal tumorigenesis is not clear. Upcoming mixture experiments will help clarify this question.

*Acknowledgements:*

RKS is grateful for support from NASA grant NNJ16H221. DWH, BS, JG, and JY are grateful for support from the UC Berkeley undergraduate research apprenticeship program (URAP). We

are grateful to Dr. E.A. Blakely, Dr. P.Y. Chang, and Dr. J.H. Mao for discussions. We thank Dr. F.A. Cucinotta and Dr. M. Hada for clarifying some details of the data sets.

**Bibliography**

*1.* Fraser TR. Lecture on the Antagonism between the Actions of Active Substances. Br Med J. 1872;2(618):485-7.

*2.* Loewe S, Muischnek H. Ueber Kombinationswirkungen. I. Mitteilung Hilfsmittel der Fragestellung. Archiv for Experimentelle Pathologie und Pharmakologie. 1926;114:313-26.

*3.* Zaider M, Rossi HH. The synergistic effects of different radiations. Radiat Res. 1980;83(3):732-9.

*4.* Fry RJ, Powers-Risius P, Alpen EL, Ainsworth EJ. High-LET radiation carcinogenesis. Radiat Res Suppl. 1985;8:S188-95.

*5.* Lam GK. The interaction of radiations of different LET. Phys Med Biol. 1987;32(10):1291-309.

*6.* Katz R. Radiobiological Modeling Based On Track Structure. Quantitative Mathematical Models in Radiation Biology, ed. J. Kiefer. 1988 [cited 2016 December]. From Kiefer Volume]. Available from: http://digitalcommons.unl.edu/physicskatz/60.

*7.* Berenbaum MC. What is synergy? Pharmacol Rev. 1989;41(2):93-141.

*8.* Brauer F, Nohel J. The Qualitative Theory of Ordinary Differential Equations. New York: Dover; 1989. 314 p.

*9.* Zaider M. Concepts for describing the interaction of two agents. Radiat Res. 1990;123(3):257-62.

*10.* Curtis SB, Townsend LW, Wilson JW, Powers-Risius P, Alpen EL, Fry RJ. Fluence-related risk coefficients using the Harderian gland data as an example. Adv Space Res. 1992;12(2-3):407-16.

*11.* Alpen EL, Powers-Risius P, Curtis SB, DeGuzman R. Tumorigenic potential of high-Z, high-LET charged-particle radiations. Radiat Res. 1993;136(3):382-91.

*12.* Lam GK. A general formulation of the concept of independent action for the combined effects of agents. Bull Math Biol. 1994;56(5):959-80.

*13.* Alpen EL, Powers-Risius P, Curtis SB, DeGuzman R, Fry RJ. Fluence-based relative biological effectiveness for charged particle carcinogenesis in mouse Harderian gland. Adv Space Res. 1994;14(10):573-81.

*14.* Binder K. Introduction: General Aspects of Computer Simulation Techniques and Their Applications in Polymer Physics. In: Binder K, editor. Monte Carlo and Molecular Dynamics Simulations in Polymer Science. Oxford: Oxford University Press; 1995.

*15.* Cucinotta FA, Nikjoo H, Goodhead DT. Applications of amorphous track models in radiation biology. Radiat Environ Biophys. 1999;38(2):81-92.

*16.* Brenner DJ, Little JB, Sachs RK. The bystander effect in radiation oncogenesis: II. A quantitative model. Radiation Research. 2001;155(3):402-8.

*17.* Zhou G, Bennett PV, Cutter NC, Sutherland BM. Proton-HZE-particle sequential dual-beam exposures increase anchorage-independent growth frequencies in primary human fibroblasts. Radiat Res. 2006;166(3):488-94.

*18.* Lorenzo JI, Sanchez-Marin P. Comments on "Isobolographic analysis for combinations of a full and partial agonist: curved isoboles". J Pharmacol Exp Ther. 2006;316(1):476-8; author reply 9.

*19.* Goodhead DT. Energy deposition stochastics and track structure: what about the target? Radiat Prot Dosimetry. 2006;122(1-4):3-15.

*20.* Chou TC. Theoretical basis, experimental design, and computerized simulation of synergism and antagonism in drug combination studies. Pharmacol Rev. 2006;58(3):621-81.

*21.* Cucinotta FA, Chappell LJ. Non-targeted effects and the dose response for heavy ion tumor induction. Mutat Res. 2010;687(1-2):49-53.

*22.* Brun YF, Greco WR. Characterization of a three-drug nonlinear mixture response model. Front Biosci (Schol Ed). 2010;2:454-67.

*23.* Boedeker W, Backhaus T. The scientific assessment of combined effects of risk factors: different approaches in experimental biosciences and epidemiology. Eur J Epidemiol. 2010;25(8):539-46.

*24.* Matloff N. The Art of R Programming. San Francisco: No Starch Press; 2011.

*25.* Tallarida RJ. Revisiting the isobole and related quantitative methods for assessing drug synergism. J Pharmacol Exp Ther. 2012;342(1):2-8.

*26.* Geary N. Understanding synergy. Am J Physiol Endocrinol Metab. 2013;304(3):E237-53.

*27.* Cucinotta FA, Kim MH, Chappell LJ. Space Radiation Cancer Risk Projections and Uncertainties – 2012. Hanover, MD; http://ston.jsc.nasa.gov/collections/TRS: NASA Center for AeroSpace Information, 2013.

*28.* Cucinotta FA, Kim MH, Chappell LJ, Huff JL. How safe is safe enough? Radiation risk for a human mission to Mars. PLoS One. 2013;8(10):e74988.

*29.* Hada M, Chappell LJ, Wang M, George KA, Cucinotta FA. Induction of chromosomal aberrations at fluences of less than one HZE particle per cell nucleus. Radiat Res. 2014;182(4):368-79.

*30.* IEEE. Inst. Electric and Electronic Engineers: Top 10 Programming Languages 2014 [03/2015]. Available from: http://spectrum.ieee.org/computing/software/top-10-programming-languages.

*31.* Piggott JJ, Townsend CR, Matthaei CD. Reconceptualizing synergism and antagonism among multiple stressors. Ecology and Evolution:. 2015;5(7):1538–47.

*32.* Tang J, Wennerberg K, Aittokallio T. What is synergy? The Saariselkä agreement revisited. Frontiers in Pharmacology. 2015;6:181.

*33.* Kim MH, Rusek A, Cucinotta FA. Issues for Simulation of Galactic Cosmic Ray Exposures for Radiobiological Research at Ground-Based Accelerators. Front Oncol. 2015;5:122.

*34.* Foucquier J, Guedj M. Analysis of drug combinations: current methodological landscape. Pharmacol Res Perspect. 2015;3(3):e00149.

*35.* Chang PY, Cucinotta FA, Bjornstad KA, Bakke J, Rosen CJ, Du N, et al. Harderian Gland Tumorigenesis: Low-Dose and LET Response. Radiat Res. 2016;185(5):449-60.

*36.* Cacao E, Hada M, Saganti PB, George KA, Cucinotta FA. Relative Biological Effectiveness of HZE Particles for Chromosomal Exchanges and Other Surrogate Cancer Risk Endpoints. PLoS One. 2016;11(4):e0153998.

*37.* Norbury JW, Schimmerling W, Slaba TC, Azzam EI, Badavi FF, Baiocco G, et al. Galactic cosmic ray simulation at the NASA Space Radiation Laboratory. Life Sci Space Res (Amst). 2016;8:38-51.

*38.* Sollazzo A, Shakeri-Manesh S, Fotouhi A, Czub J, Haghdoost S, Wojcik A. Interaction of low and high LET radiation in TK6 cells-mechanistic aspects and significance for radiation protection. J Radiol Prot. 2016;36(4):721-35.

*39.* Siranart N, Blakely EA, Cheng A, Handa N, Sachs RK. Mixed Beam Murine Harderian Gland Tumorigenesis: Predicted Dose-Effect Relationships if neither Synergism nor Antagonism Occurs. Radiat Res. 2016;186(6):577-91.

*40.* Shuryak I. Quantitative modeling of responses to chronic ionizing radiation exposure using targeted and non-targeted effects. PLoS One. 2017;12(4):e0176476.

*41.* Cucinotta FA, Cacao E. Non-Targeted Effects Models Predict Significantly Higher Mars Mission Cancer Risk than Targeted Effects Models. Sci Rep. 2017;7(1):1832.

*42.* Shuryak I, Fornace AJJ, Jr., Datta K, Suman S, Kumar S, Sachs RK, et al. Scaling Human Cancer Risks from Low LET to High LET when Dose-Effect Relationships are Complex. Radiat Res. 2017;187(4):476-82.